SULFATE IN HONG KONG

Roger Kwok*, Jimmy C.H. Fung, Alexis K.H. Lau
Institute for the Environment, Hong Kong University of Science & Technology, Kowloon, HK

Joshua S. Fu
Department of Civil & Environmental Engineering, University of Tennessee, Knoxville, TN, USA

Zion S. Wang and Gail Tonnessen
Bourns College of Engineering Center for Environmental Research and Technology, University of California at Riverside, CA, USA

1. STATEMENTS OF PROBLEM

Visibility impairment associates with particulate matter (PM) level. In Hong Kong (HK), sulfate takes up 25% of total PM concentration (Yuan et al 2006).   In the neighborhood of HK, Pearl River Delta (PRD) region has long become a densely populated metropolitan area with intense industrial and commercial activities. Now we come to wonder how much SO2, SO4, EC in HK are contributed from HK, PRD and beyond; what major emission sources are affecting HK's SO2, SO4 and EC levels? How do the pollutant levels vary from season to season? To answer these questions, we resort to a regional air quality model CMAQ, and it's variant Tagged Species Source Apportionment (TSSA) algorithm. Model setup for the basic CMAQ is described in Section 2, and subsequent results of four seasons of 2004 will be presented in Section 3. Devised by Tonnesen and Zion (2008), TSSA will be described in Section 4. Setup for HK-PRD application will also be laid out. Section 5 presents results from the TSSA in hope of revealing source contributions and reasons behind the seasonal variations.

2. MODEL CONFIGURATIONS

Model configurations, including descriptions of meteorological and emission inputs, can be referred to Kwok et al (2007). In addition, MM5 had been running with observational winds nudged at meteorological stations around HK. Waglan Island, one of the stations at southeastern waters of HK (Fig 1), is a good referencing site representing the background winds and consequently the climate of HK. The wind rose

plots in Fig 2 show that HK is subject to predominantly easterly circulations throughout the year. In particular, the region is subject to northeasterly monsoon in fall and winter of 2004. In spring and summer, the region is exposed to either easterly streams or summer monsoons from the southwest. We will demonstrate that this climatology plays an important part in seasonal variations of pollutant level in HK.
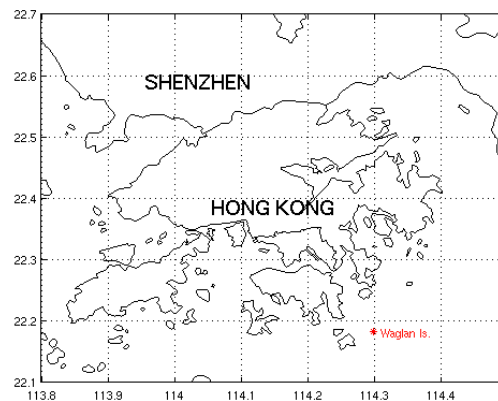

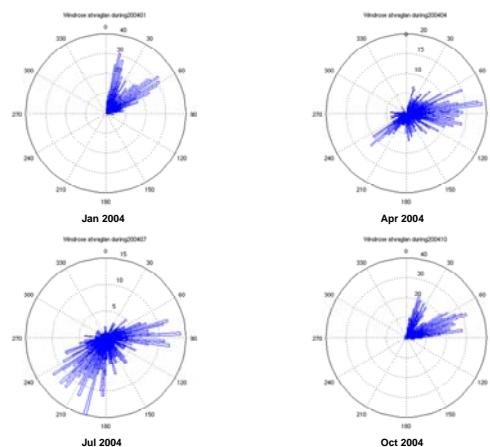Fig 1. Location of wind station at Waglan Island.

Fig 2. MM5 wind rose at Waglan Island in Jan, Apr, Jul and Oct 2004.

*Corresponding author: Roger Kwok, Institute for the Environment, Hong Kong University of Science & Technology, Clear Water Bay, Kowloon, Hong Kong; e-mail: maroger@ust.hk

In the basic run CMAQ 4.6 is used, selecting yamo scheme for advection and cb4_ae4_aq for gaseous-aqueous chemistry with AE4 module.

3. RESULTS FROM BASIC RUNS

Due to the length constraints, time series plots displayed in this section are limited to observations at an HKEPD ambient station Yuen Long (Fig 3). The choice of the station lies on its proximity to neighboring Shenzhen city in the north and PRD estuary in the west, in hope of capturing regional influences from the both sides.

Fig 3. Air quality monitoring stations maintained by Hong Kong Environmental Protection Department.

Fig 4 shows the time series of hourly model and observational fine PM sulfate concentrations for April, July and October 2004; there is no January sulfate observation. Several remarks arise from these results. First of all, average concentrations in the observed data are generally lower in July as a summer month, followed by April as a spring one. The autumnal October has the higher concentrations than all other months. Interestingly, there is a correspondence between the patterns in the wind-roses with the concentration levels for each season. For instance, the northeasterly background winds in October may be associated with the relatively higher sulfate level in that month, while the occurrence of southwesterly winds coincide with lower sulfate levels in April and July. Second remark is made on the capability of the model in terms of capturing underlying trends of, and response to the peaks of the observations. Of course, peaks are not always matched at comparable level and are sometimes either ahead of or behind the observational peaks.

But given that sulfate has residential time in days, observation-simulation lags within a day are quite acceptable.
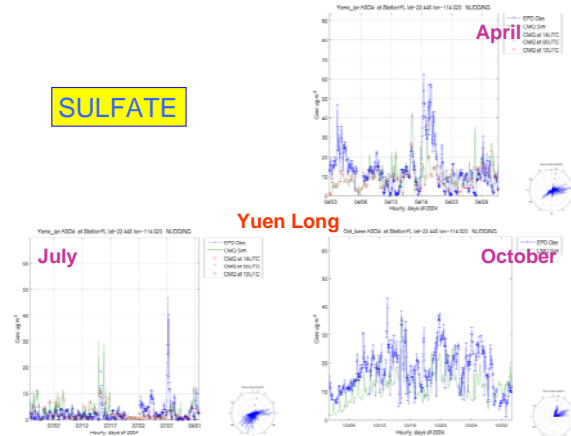

Fig 4. Observed and modeled sulfate hourly time series at Yuen Long in Apr, Jul and Oct 2004.

Fig 5 is similar to Fig 4, except that the species is SO2 and that January observations are available. Contrary to the sulfate, background concentrations are quite similar throughout the year averaged at approximately 10 ppb level. As a precursor to sulfate, SO2 only enjoy residence time in the order of hours before undergoing chemical transformations, the major pathway being aqueous. As a result, SO2 seems to always maintain its background concentration. Then the seasonal variation of sulfate cannot be explained by *local* SO2 conversion alone. This is consistent with the correspondence between seasonal wind patterns and that of the sulfate level.

As before, the model generally responds to observational peaks, although it does not always match them at comparable levels at the same hour. In January, April and October, peaks are often preceded and followed by rising and declining trends, suggesting possible influences at a bigger distance to the region. On the other hand, sudden spikes in July, preceded and followed by low flat trends, strongly suggest the importance of local sources. The background SO2 is only half of those in all other seasons, amid the ventilation effects by maritime easterly winds or southwesterly summer monsoons. In times when winds are light if not calm, heat island-induced land-sea breezes start to circulate local PM substances (Lo 2005), thus inducing isolated SO2 spikes.
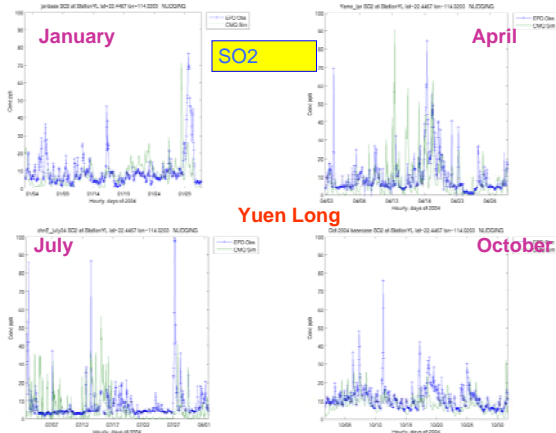
Fig 5. Observed and modeled SO2 hourly time series at Yuen Long in Jan, Apr, Jul and Oct 2004.

As a side line, comparisons are also made in OC and EC, as shown in Fig 6, though only six-day sampled measurements for speciated PM data are available at Yuen Long. Model data are taken 24-hour averages in order to compare the measurement data. Most seasons exhibits very good reproduction of OC-EC levels by the model, except for the EC in July, in which model under-predicts the measurements.
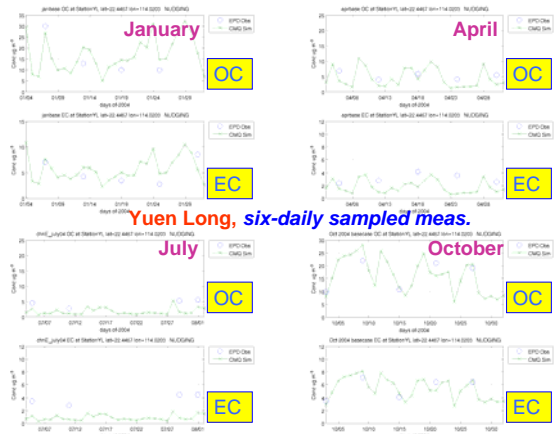

Fig 6. Six-day sampled observations and daily-averaged model time series of OC and EC at Yuen Long in Jan, Apr, Jul and Oct 2004.

In general, with realistic emission and meteorological inputs, the model is proven capable of reproducing the observational patterns in all seasons. Therefore we can further proceed to answering questions in Section 1 with an innovative method described in the next section.

4. THE TAGGING ALGORITHM

The Tagged Species Source Apportionment Algorithm (TSSA) (Tonnesen and Wang 2008) relies on the following principle.

Suppose in a usual CMAQ system we refer a "bulk concentration" to a species' instantaneous concentration within any grid cell, denoted by $C(t)$ at time t. During integration time Δt, every process $F(t)$, from advection to chemistry, updates $C(t)$ to $C(t + \Delta t)$ at subsequent time $t + \Delta t$; i.e.,

$$C(t + \Delta t) = C(t) + F(t) \qquad (1)$$

Now, TSSA assigns extra arrays in each of the grid cell. These arrays hold instantaneous concentrations as well as concentration changes from predefined individual tagged sources, named $TracerC_{j,k}(t)$ and $TracerF_{j,k}(t)$, respectively. Subscripts j and k refer to source region and source categories, respectively. Intuitively, the bulk concentration is the sum of the tagged instantaneous tracers, while the bulk processes exactly equals the tagged process tracers put together. Thus Equation (1) becomes

$$C(t + \Delta t) = \sum_{j}^{\substack{Source \\ region}} \sum_{k}^{\substack{Source \\ categories}} \left[TracerC_{j,k}(t) + TracerF_{j,k}(t) \right]$$

$$(2)$$

Equation (2) implies that emission categorization is required. Within PRD domain of grid dimension 49 x 49 with resolution at 4.5 km (D3), emissions are split up based on source category codes (SCC) in emission inventories. The inventory is divided into five sub-inventories; namely, point source, marine source, industrial source, on-road vehicular source, and all other anthropogenic and biogenic source (Fig 7).

In addition to the emissions within D3, contributions from outside D3 and from non-emitting sources must also be accounted for. Therefore boundary and initial conditions are also tagged.

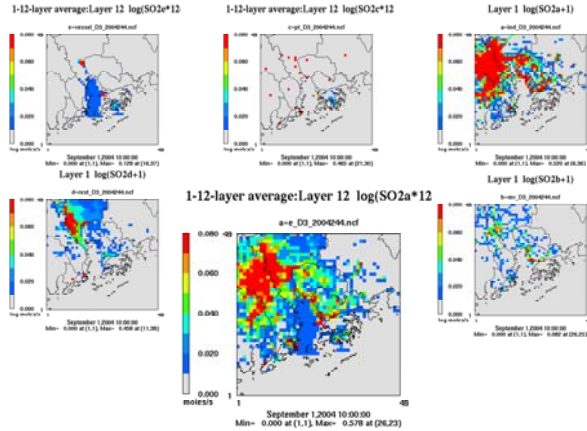TSSA also needs distinct regions to be tagged. Fig 8 displays the tagging counties within PRD.

Fig 7. PRD SO2 emissions for TSSA. Middle bottom: total. Anti-clockwise from bottom right: vehicle, industrial, point, marine and others.

In this study SO2, sulfate and EC are the tagging species. So the total number of tags is tagging species times emission categories times tagging counties plus initial and boundary conditions. Currently, TSSA is implemented in CMAQ 4.5 with yamo advection scheme and AE3 module. Results for Jan, Apr, Jul and Oct 2004 are briefly reported in the next section.
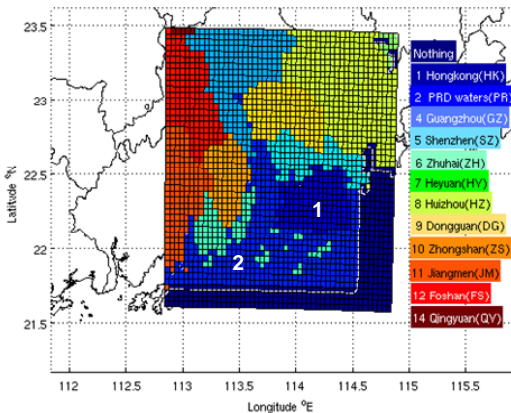

Fig 8. PRD counties as TSSA's tagged regions.

5. RESULTS FROM TSSA

All stacked bar charts presented in this section are HK domain-averaged monthly concentrations of species contributed from emission types or tagging regions. Fig 9 shows that SO2 level is higher in Jan and Oct 2004. During these two months the boundary conditions are the major contributors, accounting for over 60% of the total concentrations. Recall the wind rose in Fig 2, in which northeasterly winds prevail in these two months. Together, it becomes most likely that the

winter monsoon imports SO2 from outside the PRD region.

The next influencing SO2 contributors are point and marine sources. To see where the sources originate, stacked bar charts are also plotted in Fig 10 to display the portions contributed from individual PRD counties. It becomes evident that HK and Shenzhen point source, mainly power plants, contribute most (Fig 10(a)). Dongguan, north of Shenzhen, occasionally imports extra SO2 into HK. Marine sources, on the other hand, are shared by waters in HK, PRD estuary, and Shenzhen.
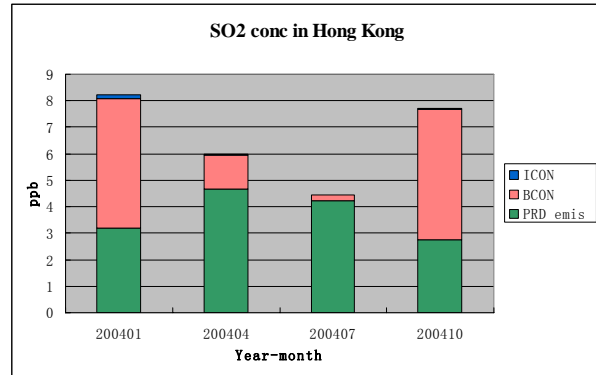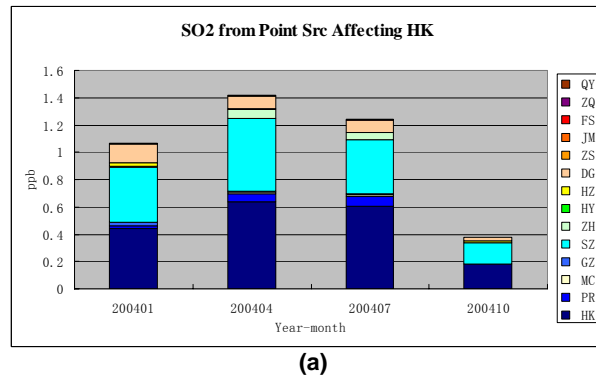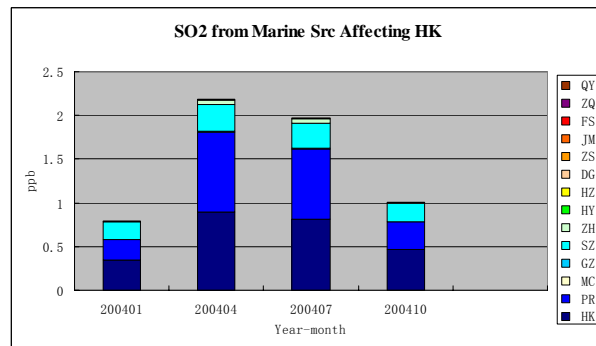

Fig 9. Average SO2 concentrations in HK from major tags for Jan, Apr, Jul and Oct 2004.

(a)

(b)

Fig 10. Regional contribution to HK SO2 of Fig 7 from (a) point source and (b) marine source.

Proportions of sulfate tags (Fig 11) look similar as those of Fig 9, except that boundary conditions are even more dominant, over 70% of total concentration in cooler seasons. This is quite reasonable since residence time of sulfate is longer than SO2, so there is enough time to get transported at a longer distance. So sulfate is undoubtedly super-regional originated.

The winter/summer contrast is even more profound and is certainly associated with the monsoon winds at different seasons.
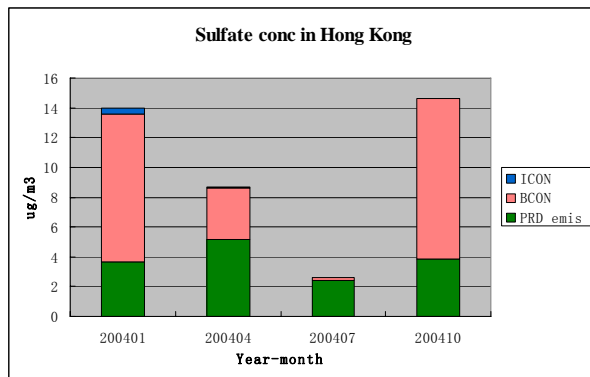

Fig 12. Average EC concentrations in HK from tagged emission types for Jan, Apr, Jul and Oct 2004.

Fig 11. Average sulfate concentrations in HK from major tags for Jan, Apr, Jul and Oct 2004.
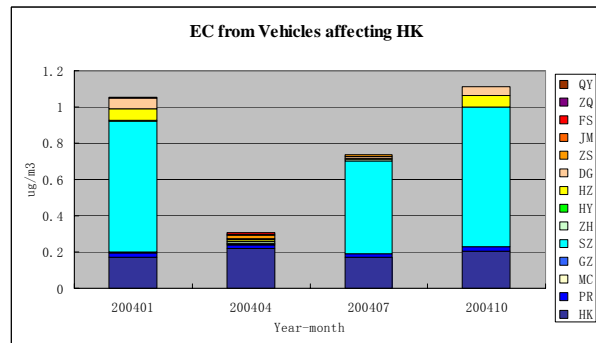
Fig 13. Regional contribution to HK EC of Fig H from vehicle source.

6. SUMMARY

EC is also included as a tagging species since it is chemically inert, and therefore it serves as a tracer. Fig 12 shows that EC carries substantial super-regional effects, owing to the climates affecting HK/PRD (Fig 2). It is note that there is only one major emission category dominating HK EC level: vehicles. And it turns out that Shenzhen vehicle EC advects to HK in most seasons except April for spring(Fig 13). Contrary, EC from HK vehicles is quite uniform throughout the year.
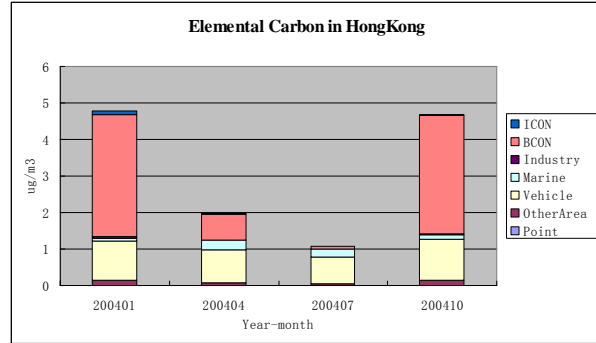
PM level in Hong Kong, including sulfate, are high in autumn and winter; and lower in spring and summer. Northeasterly monsoon due to continental outflow during the cooler seasons imports the PM from outside the PRD, while the southwesterly summer monsoon from the sea brings down the PM level. When background winds subside, local land sea-breezes due to urban heat island take over and circulate PM from regional sources within the region.

PM species are very likely contributed super-regionally in fall and winter 2004. In addition, emission sources affecting HK SO2 and sulfate levels include those from power plants and ships, while HK elemental carbon mainly comes from vehicles. In all cases, emission sources originate mostly from HK itself and neighboring Shenzhen.

7. ACKNOWLEDGMENT

8. REFERENCES

Kwok, H.F.R., J.C.H. Fung, A.K.H. Lau and J.S. Fu 2007: Urban effects of Hong Kong and Pearl River Delta region on sulfur cycle. *6-th Annual CMAS Conference, UNC Chapel Hill, NC, Oct 1-3 2007.*

Lo, J.C.F, Lau, A.K.H., Fung, J.C.H., and Chen, F., 2006: Investigation of enhanced cross-city transport and trapping of air pollutants by coastal and urban land-sea breeze curculations. J.Geophys. Res, 111, D14104, doi:10.1029/2005JD006837.

Tonnesen, G.S. and Z.S. Wang, 2008: Development of a Tagged Species Source Apprtionment Algorithm (TSSA) to characterize 3-dimensional transport and transformation of precursors and secondary pollutants. To be published.

Yuan, Z., A.K.H. Lau, H. Zhang, J. Yu, P.K.K. Louie and J.C.H. Fung, 2006: Identification and spatiotemporal variations of dominant PM10 sources over Hong Kong. Atmos Env., 40(10), pp 1803-1815. doi:10.1016/j.atmosenv.2005.11.030